24th INTERNATIONAL CONGRESS ON SOUND AND VIBRATION
23–27 July 2017, London

ICSV24
23-27JULY 2017
LONDON CALLING

ANALYSIS OF GEAR DYNAMICS OF A HELICAL GEAR PAIR WITH FAULTS

Y.M. Huang and K.Y. Huang

Department of Mechanical Engineering, National Central University, Chungli, Taiwan
email: t330005@cc.ncu.edu.tw

This paper presents the dynamic responses of a helical gear pair. The goal of the research provides information for diagnosing the gear faults through examining dynamic signals. Gear faults including crack and spalling on one tooth were considered. A finite element software, ANSYS, was chosen to calculate the gear mesh stiffness for both an undamaged gear pair and gear pairs with faults. A dynamic, lumped-parameter model of gear pairs was then developed for the system responses. The presented model considers not only the gear with fault, but also an unbalanced gear. Two signal processing methods, fast Fourier analysis and cepstrum analysis, were introduced to find the characteristics of the dynamic responses of an undamaged gear pair and gear pairs with various faults. The difference between two types of responses was then identified. An experiment was conducted to obtain data for comparison.

This paper concludes that a fault in the gear can result in small components in the frequency domain with the interval equal to the rotating speed of the faulted gear. This feature can be further clearly identified in the cepstrum domain and can provide a good evidence of a gear pair with faults.

Keywords: helical gear pair, gear fault diagnosis, FEM, dynamic response

1. Introduction

This paper discusses the dynamic responses and their characteristics of an undamaged pair or gear pairs with faults. The gear pair is used in a 150 kW wind turbine. The mesh stiffness of a gear pair were obtained by using finite element software. Then, a lumped dynamic model of a gear pair was derived. The mesh stiffness was introduced into the model. The dynamic responses of an undamaged gear pair and several faulted gear pairs were calculated. The research can distinct the difference of the two types of responses and provide diagnosis guidelines. Experimental results were also discussed.

Many references, investigating the dynamics of gear pairs, can be found. An earlier paper [1] studied gear dynamics based on experimental observations. The behavior of spur gears at low speeds could be described using static transmission error curves which relate to the forces between teeth at any instant. Ozguven and Houser [2] reviewed different mathematical models for analyzing gears. In two later papers [3,4], theoretical models of the spur and helical gears were developed. The static transmission errors of gear pairs of meshing were discussed. The gear dynamics can also be found by using the finite element method. Related papers were [5,6,7]. These researchers meshed the entire gear pair for the time-consuming analysis. Some researchers then chose to use the finite element method only for the mesh stiffness between gears [8]. This approach can also be employed in finding the mesh stiffness of damaged gears [8,9]. Chaari, et al., have studied the problems of mesh stiffness of gears with faults by using springs connected in parallel and series [10,11]. The mesh stiffness can be included in the dynamic model of a gear pair for calculating the dynamic response [8]. The resulted time responses were analyzed by different approaches [12,13]. In our research, the spectrum and the cepstrum [12] of the dynamic responses were investigated and discussed.

2. Mesh stiffness

2.1 Finite element analysis

A finite element software, ANSYS, was used to calculate the mesh stiffness of a helical gear pair. We focused on the difference between the undamaged and the damaged pairs.

The mesh stiffness between two gears consists several springs connected in series [10,11,14] as given in Fig. 1. The total stiffness (k_{gi}) of each gear (Fig. 1(a)) is the combination of the torsional stiffness $k_{i,T}$ of base circle, the bending stiffness $k_{i,B}$ of the tooth, and the stiffness $k_{i,C}$ from Hertz contact of two gears where i =1 or 2 is the gear number. If more than one contact pair exists, the mesh stiffness becomes the effect of all mesh stiffness (K_1 and K_2 in Fig. 1(b)) of contact pairs connected in series.

To obtain the static mesh stiffness using ANSYS, one needs two steps. First, choose a fixed boundary at gear 1 and apply an external torsional torque to gear 2. The stiffness of gear 1 is then determined using $k_{g1} = F / x_1$ where F is the equivalent applied force and x_1 is the normal deflection at the contact point of gear 1. In the second step, the fixed boundary and the point of applied external torque are reversed to find the stiffness k_{g2} of gear 2. Two gear stiffnesses combined together give the mesh stiffness K_j.

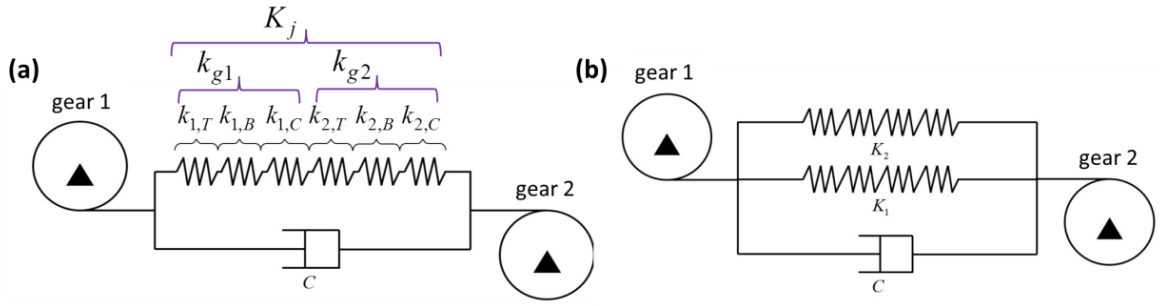

Figure 1: Mesh stiffness (a) one contact pair (b) two contact pairs

We considered a helical gear pair (Fig. 2), used in a 150kW wind turbine, with modulus 8, pressure angle 20^o, and width of tooth 140 mm. The gear has pitch radius 280 mm and 72 teeth. The pinion has pitch radius 72 mm and 18 teeth.

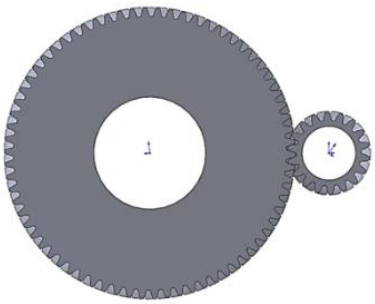

Figure 2: The helical gear pair

2.2 Mesh stiffness

The values of stiffness for various rotating speeds of the gears are given in Fig. 3. The rotating speed can affect the stiffness in a nonlinear way because of the nonlinear behavior of Hertz contact. Different rotating speeds result in different values of stiffness where a larger speed usually yields smaller stiffness probability due to the shorter contacting duration.

We considered mesh stiffnesses of an undamaged helical gear pair and gear pairs with some faults, crack (Fig. 4(a)) and spalling (Fig. 4(b)) in one tooth of the gear. Figure 5 shows the mesh stiffness for rotating speed of the gear being 35rpm. In the figure, the horizontal axis is the

contacting angle of the gear indicating the complete mesh process of one faulted tooth in the gear. Figure 5(a) gives the results with a crack in one tooth of the gear. The stiffness varies with the angle and decreases when the crack length increased from 2 mm to 11 mm. The maximum decrease about 20% occurs when contacting angle is near 3.08°. Figure 5(b) gives the results with spall in one tooth. The stiffness becomes smaller only when the angle between 1.6° and 3.6°. The maximum decrease is about 23% near the middle of the mesh process.

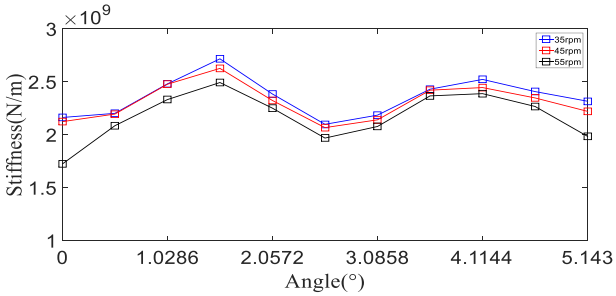

Figure 3: Mesh stiffness from ANSYS for various rotating speeds

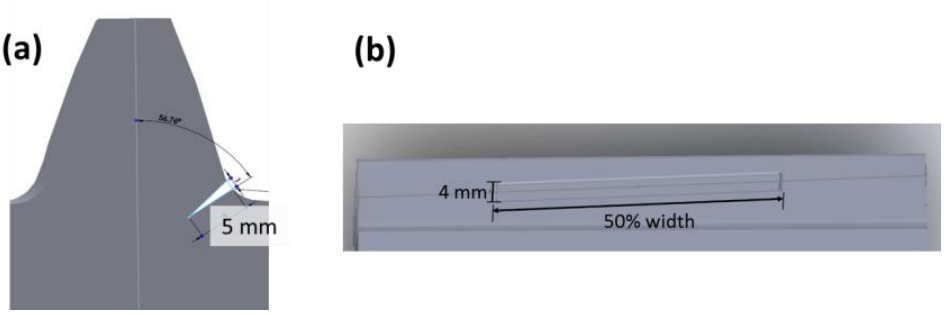

Figure 4: Faulted gear (a) with a 5 mm crack (b) with 50% spall

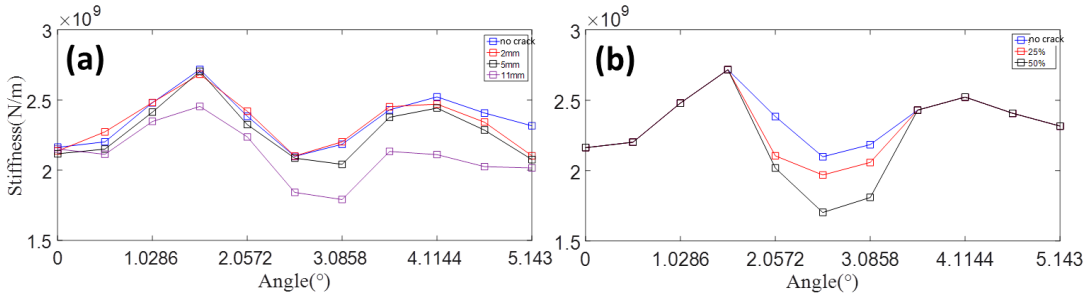

Figure 5: Mesh stiffness from ANSYS for rotating speed 35rpm
(a) with a crack in one tooth (b) with spall in one tooth

3. Dynamic model of the helical gear pair

A lumped model of the helical gear pair was developed for analyzing the dynamic characteristics of gear pairs and is shown in Fig. 6 where Fig. 6(a) is the simplified model and Fig. 6(b) is the model including the unbalance effect. In this model, we considered the inertia (I_1, I_2, and m_2) of the gear and the pinion. The radii of the gear and the pinion are r_{b1} and r_{b2}, respectively. The rotation angles are θ_1 and θ_2 where T_1 and T_2 are applied torques. The spring $k_1(\theta_1)$ represents the total mesh stiffness of the gear pair and some damping c_1 is added. The mesh stiffness in the faulted case is used when the faulted tooth of the gear in contact with the pinion. On the contrary, the stiffness in the case of no crack is used when the contacting teeth are normal. For including the effect of unbalance, we also introduced the translational displacement x_2 of the center of the pinion. Besides, an additional spring k_2 and a damping c_2 are also connected to the pinion. The spring k_2 can

be chosen as a function of displacements for evaluating the unbalance effect. The equations of motion of the model then becomes

$$\begin{cases} I_1\dfrac{d^2\theta_1}{dt^2}+c_1r_{b1}\left(r_{b1}\dfrac{d\theta_1}{dt}-r_{b2}\dfrac{d\theta_2}{dt}+\dot{x}_2\right)+r_{b1}k_1(\theta_1)(r_{b1}\theta_1-r_{b2}\theta_2+x_2)=T_1 \\ I_2\dfrac{d^2\theta_2}{dt^2}+c_1r_{b2}\left(-r_{b1}\dfrac{d\theta_1}{dt}+r_{b2}\dfrac{d\theta_2}{dt}-\dot{x}_2\right)+r_{b2}k_1(\theta_1)(-r_{b1}\theta_1+r_{b2}\theta_2-x_2)=-T_2 \\ m_2\dfrac{d^2x_2}{dt^2}+\left[c_1r_{b1}\dfrac{d\theta_1}{dt}-c_1r_{b2}\dfrac{d\theta_2}{dt}+(c_1+c_2)\dot{x}_2\right]+k_1(\theta_1)(r_{b1}\theta_1-r_{b2}\theta_2+x_2)+k_2(\theta_2)x_2=0 \end{cases} \quad (1)$$

One significant parameter in this model is the dynamic transmission error, the equivalent deflection of the mesh stiffness, defined by $x=x_2+(\theta_1 r_{b1}-\theta_2 r_{b2})$. If no unbalance effect considered, one can just set $x_2=0$. On the contrary, the spring k_2 was chosen a function of θ_2 to induce the time-dependent spring with the same period as the rotating speed of the pinion for including the effect of unbalance of the pinion.

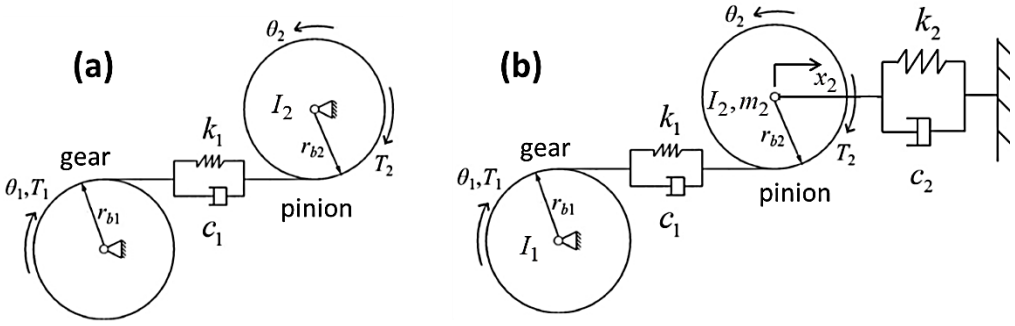

Figure 6: Dynamic model of a gear pair
(a) model without unbalance (b) model with unbalance in the pinion

3.1 Dynamic responses

The Dynamic Transmission Error (DTE) $x(t)$ for different situations are shown in Fig. 7 where no unbalance effect is considered. Figure 7(a) gives the Fourier spectrum of a gear pair with no damage. Three peaks are corresponding to the mesh frequency f_m, defined as the rotating speed times the number of teeth of the gear or pinion, and its harmonics. The second harmonic is the most significant one mainly due to the waveform of the mesh stiffness [15]. Figure 7(b) gives the Fourier spectrum of a gear with 50% spalling. Three peaks are similar to those in Fig. 7(a). However, some additional small peaks in the low frequency region are found and their frequency interval is exactly the rotating frequency $f_{\omega 1}$ of the faulted gear. This phenomenon evidences the existence of faults in the gear. Figure 7(c) and (d) show the spectrum from gears with cracks. These two figures are also similar to Fig. 7 (a) but the small peaks in the low frequency region are more obvious when the crack is longer. From the data given in Fig. 7, one cannot easily distinguish whether the gear system is damaged or not since the small peaks in the low frequency region are easy to neglect.

Another spectrum, the cepstrum, was then introduced to identify faulted gears. Cepstrum is defined as

$$C(\tau)=\left|\mathscr{F}\{\log F_{xx}(f)\}\right|^2 \quad (2)$$

where F_{xx} is the power spectrum of the signal $f(t)$ and $\mathscr{F}$ is the Fourier transform operator [12]. Therefore, cepstrum is also called "spectrum of spectrum". Cepstrum can emphasize the small frequency interval of peaks or sidebands in the Fourier spectrum. In our research, cepstrum can strongly highlight the frequency interval of small peaks in the low frequency region. Figure 8 shows the data of cepstrum for various faulted cases without any unbalance. The horizontal axis in Fig. 8

is the quefrency with the unit second (s) and Quefrency is the reciprocal of frequency in Hz. Figure 8(a) shows the cepstrum of a gear pair with no fault where no significant peak observed except many peaks in the low quefrency domain. They are corresponding to $q_m = 1/f_m$ and its harmonics. The related components, corresponding to mesh frequency f_m, are inherent in the Fourier spectrum in Fig. 7(a). Figure 8(b) gives the cepstrum of a gear with 50% spalling. One can still observe peaks in the low quefrency range corresponding to q_m and its harmonics. Two more significant peaks, corresponding to $q_{\omega 1} = 1/f_{\omega 1}$ and the first harmonic, are found and indicate the fault in the gear. Note that the spectrum, Fig. 7(b), also shows small and unobvious components with frequency $f_{\omega 1}$ in the low frequency region. Figure 8(c) and (d) give the cepstrum of gears with cracks. These figures are similar to Fig. 8(a) except some difference in the height of the peaks. Compared all figures in Fig.8, any fault in the gear introduces obvious peaks at $q_{\omega 1}$. On the other hand, the cepstrum of systems with various faults are insensitive to the type or the severity of the faults.

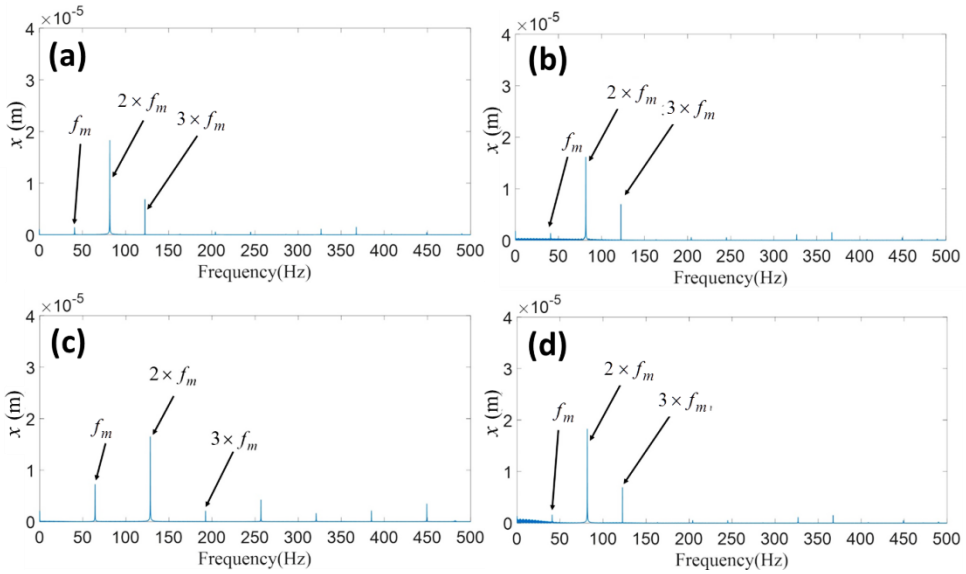

Figure 7: Fourier spectrum of DTE $x(t)$ for rotating speed 35rpm
(a) undamaged gear (b) with 50% spall in one tooth
(c) with 2 mm crack (d) 11 mm crack

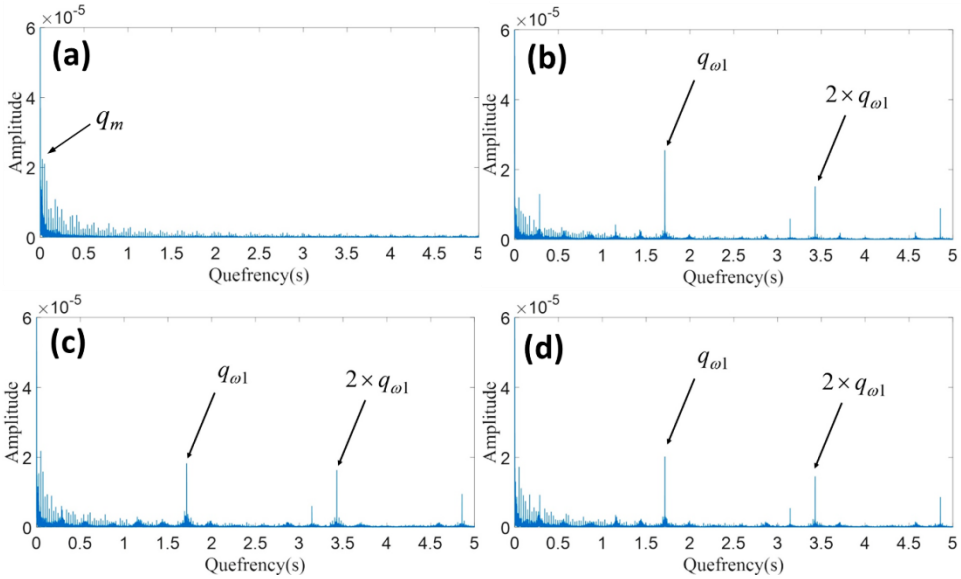

Figure 8: Cepstrum of DTE $x(t)$ for rotating speed 35rpm, balanced system
(a) undamaged gear (b) with 50% spall in one tooth
(c) with 2 mm crack (d) 11 mm crack

3.2 Dynamic responses of the system with an unbalanced axis

For studying the dynamic responses of a gear pair with unbalance, we introduced unbalance of the pinion by adding one more degree of freedom x_2 in the lumped model (Fig. 6(b)). Instead of setting an unbalance mass, we added an angle-dependent stiffness $k_2(\theta_2)$. This stiffness was chosen to become 75%, for a small interval of time, of the original value whenever the opinion makes a complete turn. This setting brought an effect similar to unbalance and gave an extra excitation with the frequency $f_{\omega 2}$ same as the rotating speed of the pinion.

The dynamic responses of a unbalance system are shown in Fig. 9. The spectrum and the cepstrum of an undamaged gear pair are in Fig. 9(a) and (c). There is no sign of unbalance, such as the peak corresponding to $f_{\omega 2}$, observed in the spectrum (Fig. 9(a)). However, the peaks corresponding to $q_{\omega 2} = 1/f_{\omega 2}$ and the harmonics are evident in the cepstrum (Fig. 9(c)). The spectrum and the cepstrum of a gear pair with spalling and unbalance are in Fig. 9(b) and (d). The spectrum (Fig. 9(b)) seems almost identical to that of an undamaged gear pair where still no peak related to unbalance effect. However, the cepstrum (Fig. 9(d)) shows peaks corresponding to both $q_{\omega 1} = 1/f_{\omega 1}$ and $q_{\omega 2} = 1/f_{\omega 2}$ along with their harmonics. The peaks associated to $q_{\omega 1}$ are due to the spall in the gear while the ones associated to $q_{\omega 2}$ resulted from the unbalance. Besides, one strong peak corresponding to $q_{\omega 12}$, the least common multiple of $q_{\omega 1}$ and $q_{\omega 2}$, is observed, indicating the interaction of spalling and unbalance.

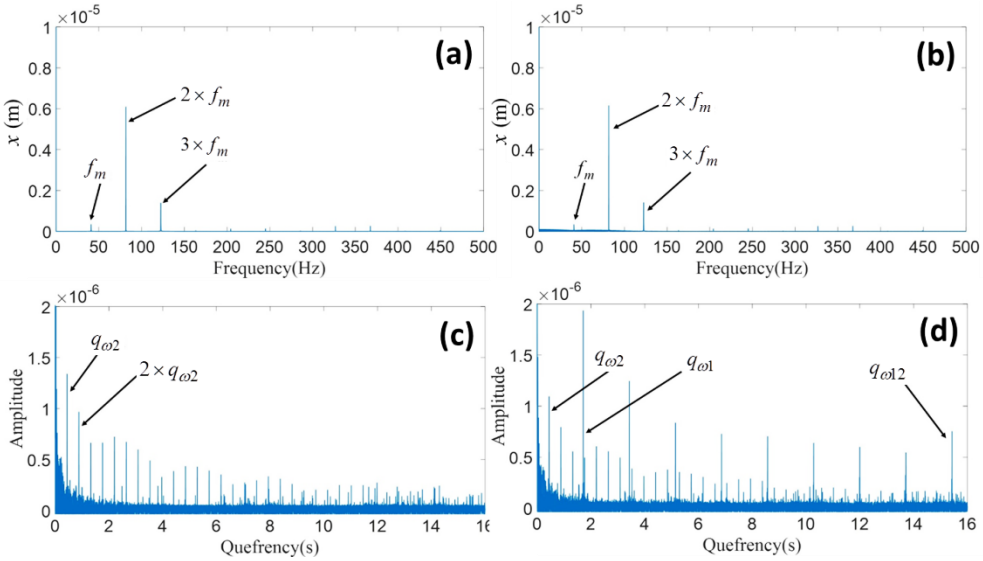

Figure 9: Numerical results of DTE $x(t)$ for rotating speed 35rpm, unbalanced system
(a) spectrum of undamaged gear (b) spectrum of gear with 50% spall
(c) cepstrum of undamaged gear (d) cepstrum of gear with 50% spall

4. Experiment and the results

An experiment was conducted to provide the comparison. Since the gear pair discussed in the previous section is designated to use in an actual wind turbine, the sizes of gears are quite large. Smaller helical gears, made by KHK, were then chosen for the experiment. The helical gears are with modulus 2, pressure angle 20°, and width of tooth 25 mm. The gear has pitch radius 41.41 mm and 40 teeth. The pinion has pitch radius 31.06 mm and 30 teeth. A picture of the test machine is given in Fig. 10(a) where a blue accelerator was attached to a position near the gear (Fig. 10(b)). Serval gears with a crack (Fig. 10(c)) or spalling (Fig. 10(d)) were fabricated for simulating the faults.

The measured accelerations are shown in Fig. 11. Figures 11(a) and (c) give the spectrum and the cepstrum of acceleration of an undamaged gear. One can find a peak and the harmonics, in the spectrum (Fig. 11(a)), corresponding to the mesh frequency f_m and also a strong peak which is near one of the natural frequencies of the system. On the other hand, in the cepstrum (Fig. 11(c)), only peaks related to $q_{\omega 1}$, $q_{\omega 2}$, and $q_{\omega 12}$ were observed. The system without any fault still generates peaks near $q_{\omega 1}$ and $q_{\omega 2}$ because of the unbalance of both the gear and the pinion unfortunately existing in our experiment. Therefore, the signs of faulted gear, the component and the harmonics corresponding to frequency $f_{\omega 1}$, were masked by the unbalance effect and not able to be observed in the spectrum and the cepstrum (Fig. 11(b) and (d)) of the gear with spall.

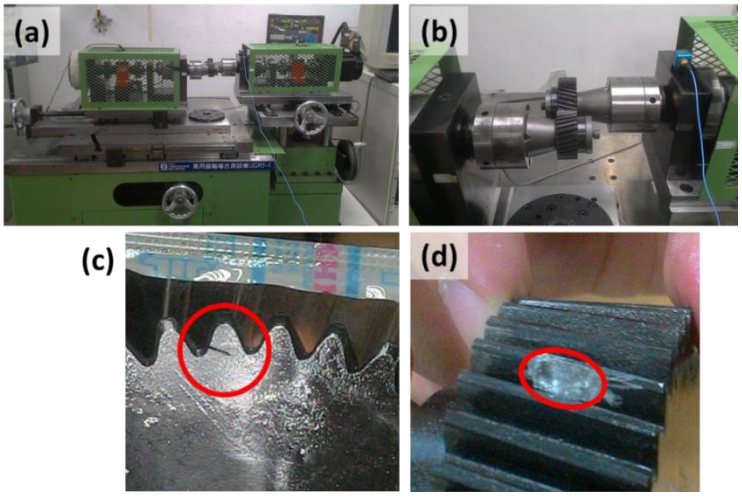

Figure 10: Experiment setup
(a) The test machine (b) gear, pinion, and the accelerator
(b) a crack in one tooth (c) spall in one tooth

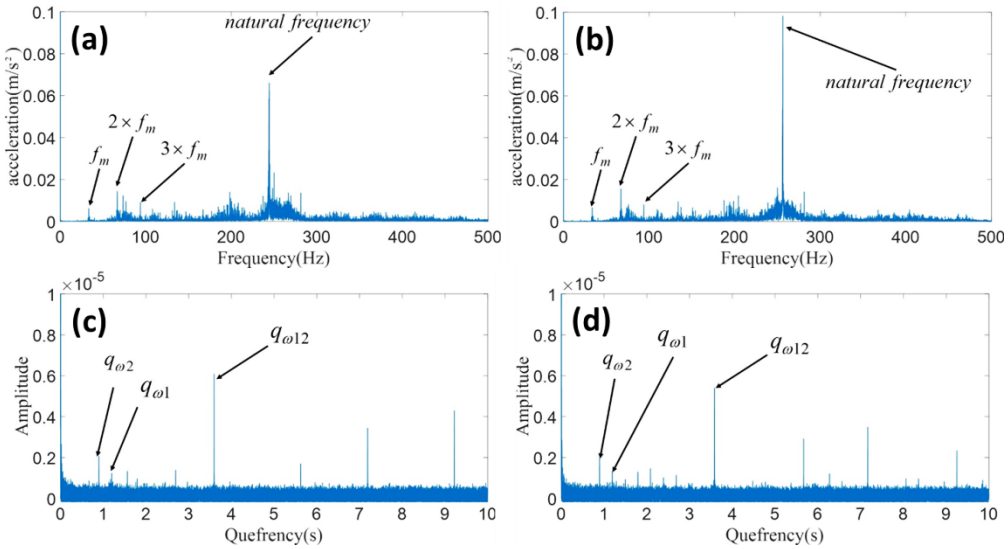

Figure 11: Experimental results of acceleration for rotating speed 50rpm
(a) spectrum of undamaged gear (b) spectrum of gear with 25% spall
(c) cepstrum of undamaged gear (d) cepstrum of gear with 25% spall

5. Conclusions

This work studied the dynamic responses of a helical gear pair with a faulted tooth in the gear. The faults discussed here were a crack or spalling in the gear. The mesh stiffness of the gear pair was calculated by finite element software, ANSYS. A lumped dynamic model, with two rotating

inertia connected by the mesh stiffness, of the gear pair was analyzed. The dynamic responses of undamaged or faulted systems were solved and discussed. The faulted gear pair can be identified by observing the cepstrum of dynamic responses. Experiments were also conducted and the results were discussed.

The following conclusions are reported.

1. The fault in a tooth of the gear can result in the reduction of mesh stiffness.
2. The change of mesh stiffness, due to gear fault, yields additional small peaks near the low frequency region in the spectrum of dynamic response. The frequency interval of these small peaks is the rotating speed of the faulted gear. However, the peaks are too tiny to be clearly observed.
3. In the cepstrum of the dynamic response, a strong peak and its harmonics, corresponding to the quefrency related to rotating speed of the faulted gear, are found. These peaks evidence the existence of the faulted tooth in the gear.
4. Unbalance brings additional peaks at the quefrency related to rotating speed of the unbalanced gear.
5. Observing the cepstrum can serve better than the spectrum for finding any faulted condition in the gear pair.

REFERENCES

1 Gregory, R. W., Harris, S. L., and Munro, R. G., "Dynamic behaviour of spur gears", *Proceedings of the Institution of Mechanical Engineers*, **178**, 207-218 (1963).

2 Ozguven, H. N. and Houser, D. R., "Mathematical models used in gear dynamics - a review", *Journal of Sound and Vibration*, **121**, 383-411 (1988).

3 Mark, W. D., "Analysis of the vibratory excitation of gear systems: basic theory", *Journal of American Acoustical Society*, **63**, 1409-1430 (1978).

4 Mark, W. D., "Analysis of the vibratory excitation of gear systems II: Tooth error representations, approximations, and application", *Journal of American Acoustical Society*, **66**, 1758-1787 (1979).

5 Parker, R. G., Vijayakar, S. M., and Imajo, T., "Non-linear dynamic response of a spur gear pair: modeling and experimental comparisons", *Journal of Sound and Vibration*, **237**, 435-455 (2000).

6 Ambarisha, V. K., and Parker, R. G., "Nonlinear dynamics of planetary gears using analytical and finite element models", *Journal of Sound and Vibration*, **302**, 577-595 (2007).

7 Cooley, C. G., Parker, R. G. and Vijayakar, S. M., "A frequency domain finite element approach for three dimensional gear dynamics", *Journal of Vibration and Acoustics*, **133** (2011).

8 Howard, I. and Jia, S., "The dynamic modeling of spur gear in mesh including friction and a crack", *Mechanical System and Signal Processing*, **15**, 831-853 (2001).

9 Jia, S., and Howard, I., "Comparison of localised spalling and crack damage from dynamic modelling of spur gear vibrations", *Mechanical Systems and Signal Processing*, **20**, 332-349 (2006).

10 Chaari, F., Baccar, W., and Haddar, M., "Effect of spalling or tooth breakage on gearmesh stiffness and dynamic response of a one-stage spur gear transmission", *European Journal of Mechanics A/Solids*, **27**, 691-705 (2008).

11 Chaari, F., Fakhfakh, T., and Haddar M., "Analytical modelling of spur gear tooth crack and influence on gearmesh stiffness", European Journal of Mechanics A/Solids, **28**, 461-468 (2009).

12 Randall, R. B., "A new method of modeling gear faults", *Journal of Mechanical Design*, 104, 259-267 (1982).

13 Bajrić, R., Sprečić, D., and Zuber, N., "Review of vibration signal processing techniques towards gear pairs damage identification", *International Journal of Engineering & Technology*, **11**, 124-128 (2011).

14 Kiekbusch, T., Sappok, D., Sauer, B., and Howard, I., "Calculation of the combined torsional mesh stiffness of spur gears with two- and three-dimensional parametrical FE models", *Journal of Mechanical Engineering*, **57**, 810-818 (2011).

15 Hedlund, J., and Lehtovaara, A., "A parameterized numerical model for the evaluation of gear mesh stiffness variation of a helical gear pair", *Journal of Mechanical Science*, **222**, 1321-1327 (2008).